Neotectonic architecture, model, and the active Longitudinal Valley suture of Taiwan

J. Bruce H. Shyu[1], Kerry Sieh[1], Yue-Gau Chen[2], Ling-Ho Chung[2], Jean-Philippe Avouac[1], Yu Wang[1,2], Ray Y. Chuang[2], and Wen-Shan Chen[2]

1: Tectonics Observatory, California Institute of Technology; 2: Department of Geosciences, National Taiwan University

A. Neotectonic architecture and the tandem suturing model of Taiwan

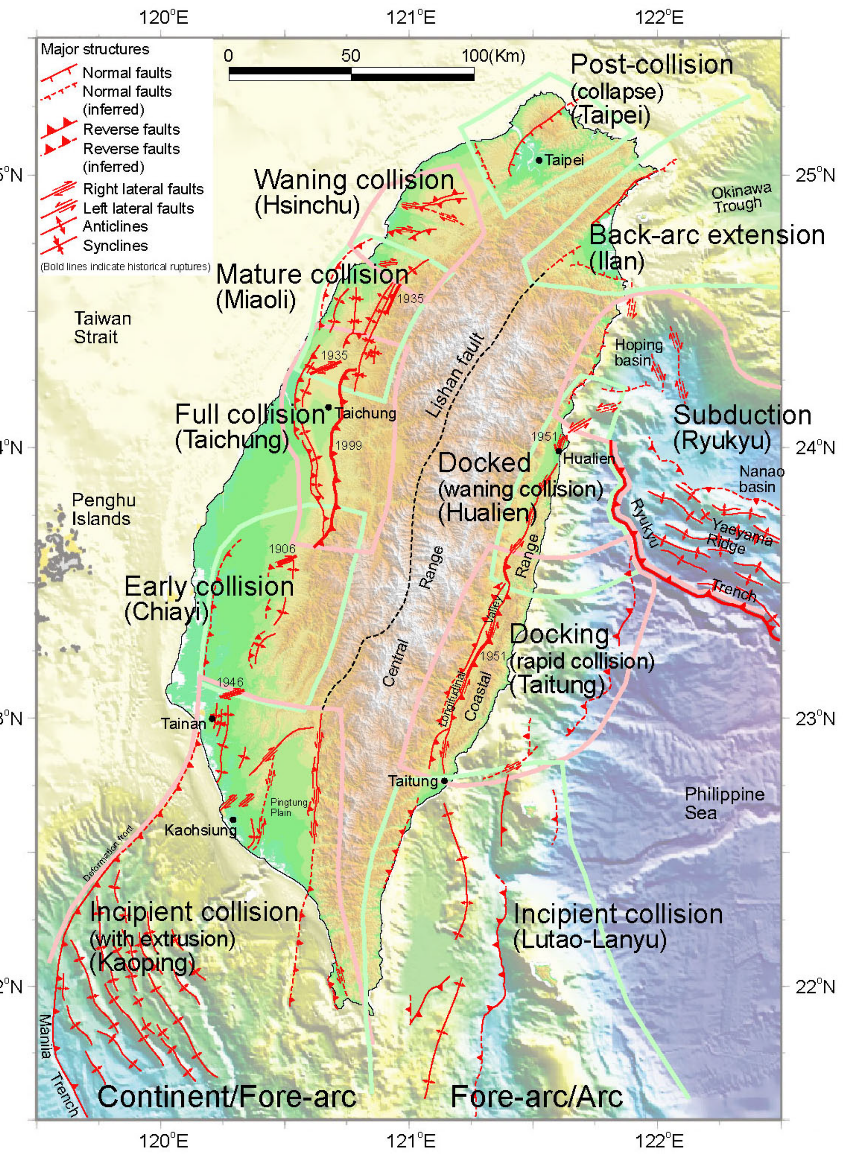

Figure A1. Map of major active faults and folds of Taiwan (in red) shows that the two sutures are producing separate western and eastern neotectonic belts. Each collision belt matures and then decays progressively from south to north. This occurs in discrete steps, manifested as 7 distinct neotectonic domains along the western belt and 4 along the eastern. A particular assemblage of active structures defines each domain. For example, two principal structures dominate the Taichung Domain. Rupture in 1999 of one of these, the Chelungpu fault, caused the disastrous Chi-Chi earthquake. The black structure that runs between the Kaoping and Ilan Domains is the suture between forearc ridge and continental margin.

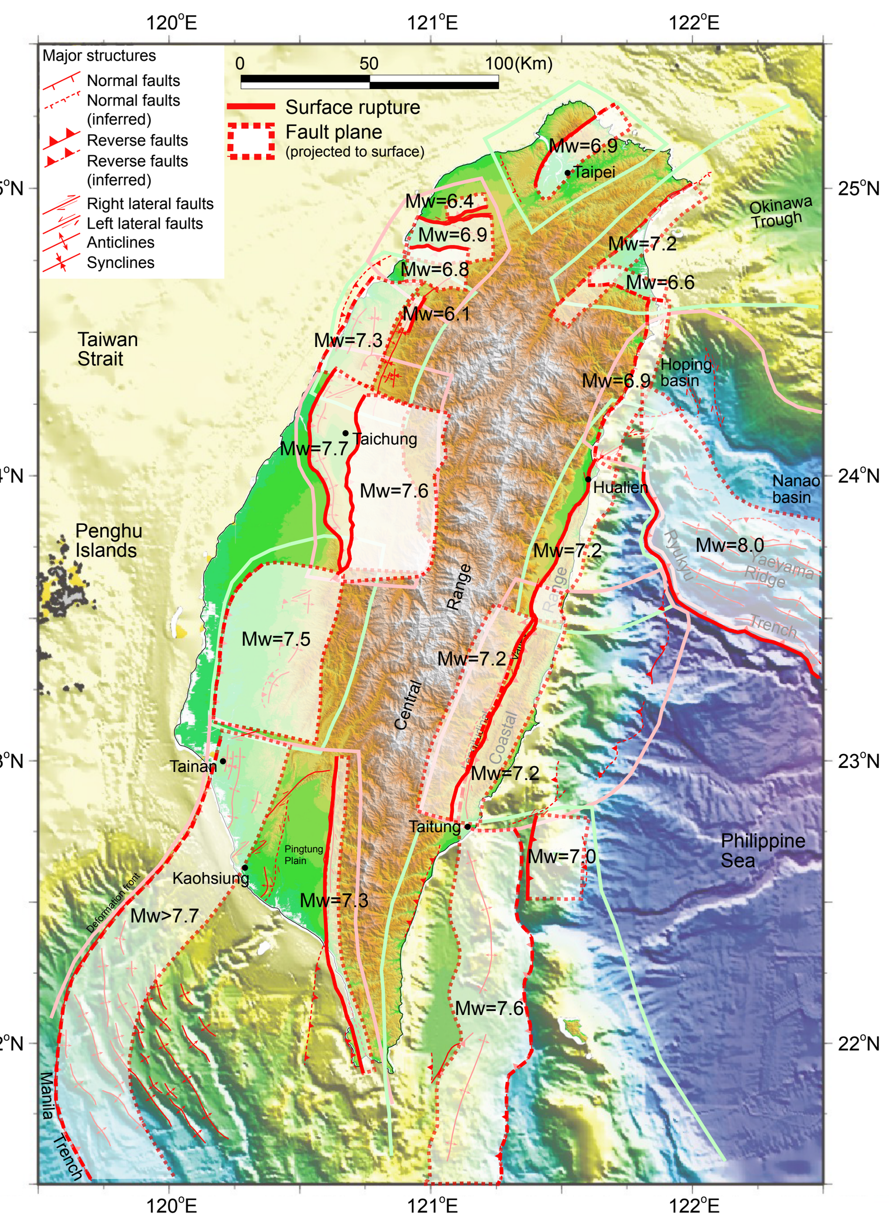

Figure A2. Proposed major sources for future large earthquakes in and around Taiwan. Bold red lines are proposed future ruptures, and the white patches are rupture planes projected to the surface. Here we have selected only a few representative scenarios to show in this figure. Earthquake magnitude of each scenario is predicted value from our calculation.

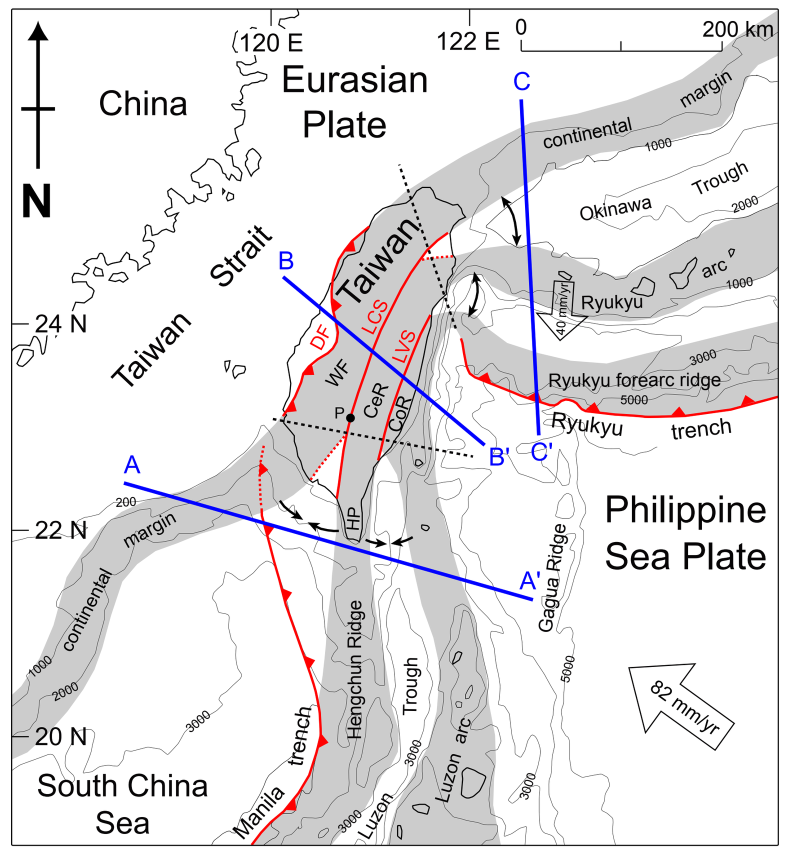

Figure A3. Taiwan is experiencing a tandem suturing of a volcanic arc and a sliver of continental crust to continental margin. In the south, the Luzon volcanic arc is converging on the Hengchun forearc ridge, which is, in turn, converging on the Chinese continental margin. Suturing of these three elements occurs in the middle of the island. In the north, both sutures are disarticulating, to form both the Okinawa Trough and troughs south of the Ryukyu island arc. Black dashed lines are the northern and western limits of the Wadati-Benioff zone of the two subducting systems, taken from the seismicity database of the Central Weather Bureau, Taiwan. Bold lines indicate cross-sections of Figure 4. DF: deformation front; LCS: Lishan-Chaochou suture; LVS: Longitudinal Valley suture; WF: Western Foothills; CeR: Central Range; CoR: Coastal Range; HP: Hengchun Peninsula; P: Outcrops of pillow lava along the western suture.

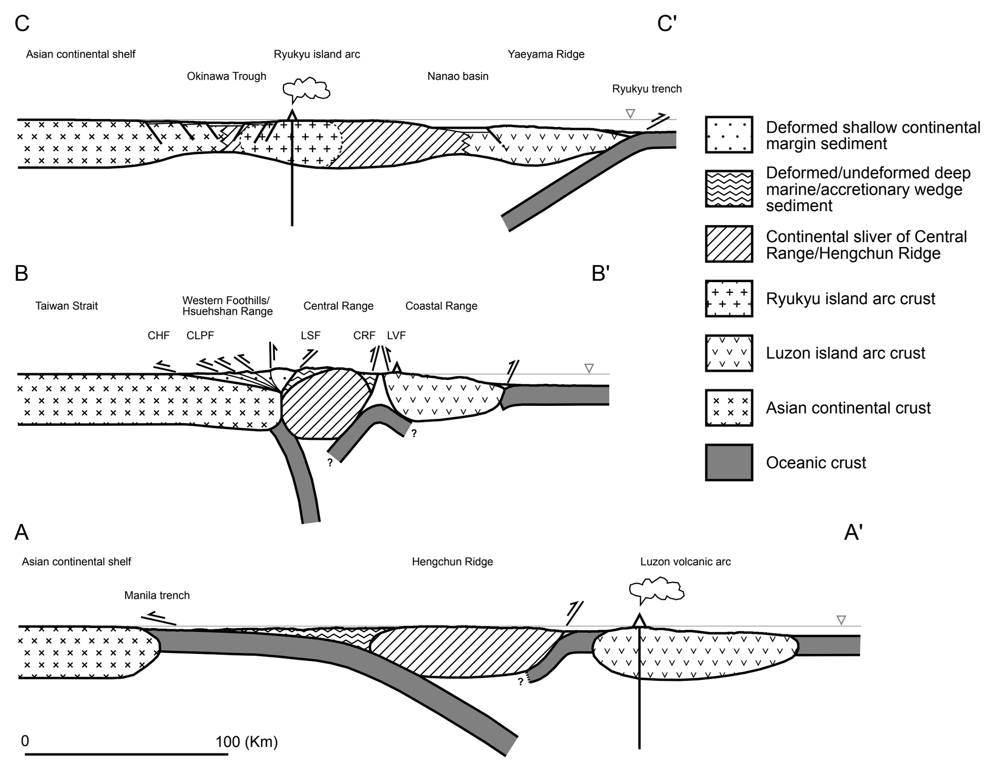

Figure A4. Three schematic crustal cross-sections across Taiwan illustrate three stages in the process of tandem suturing and disengagement. Locations of the sections are shown in Figure 3. A. Section just south of Taiwan shows the final stages of subduction and consumption of oceanic lithosphere between the three buoyant terranes. B. Section across central Taiwan shows relationship of the three terranes during suturing. C. Section north and east of Taiwan shows the subduction of the Philippine Sea plate and disengagement of the three terranes across the sutures. CHF: Changhua fault; CLPF: Chelungpu fault; LSF: Lishan fault; CRF: Central Range fault; LVF: Longitudinal Valley fault. No vertical exaggeration.

B. The Longitudinal Valley suture in eastern Taiwan: Characteristics of its major structures and the evolution of the suture

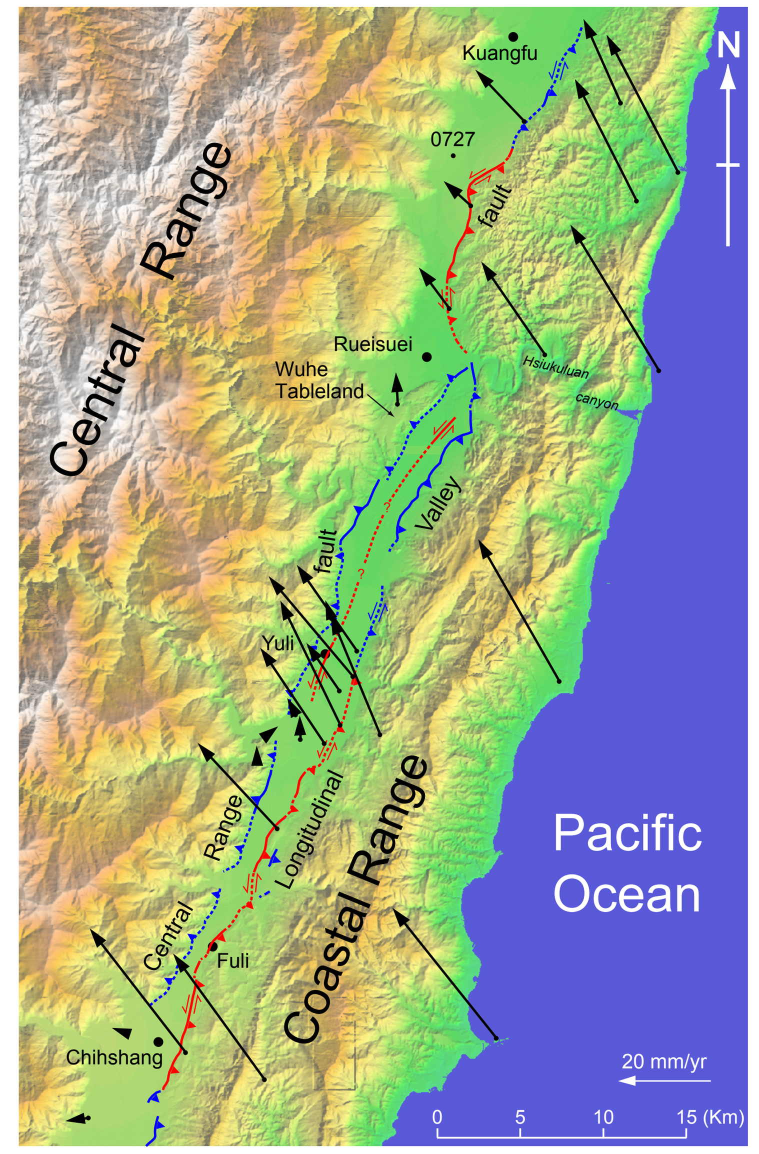

Figure B1. Map of major structures in the middle part of the Longitudinal Valley. The Longitudinal Valley fault is an east-dipping, obliquely slipping reverse fault, along which the Coastal Range is rising rapidly and moving toward the Central Range. The less prominent Central Range fault is a west-dipping reverse fault, above which many fluvial terraces and the Wuhe Tableland are rising slowly. Faults that ruptured during the 1951 earthquakes are colored red. Major faults and flexures that did not rupture in 1951 but are known to be active are colored blue. Black arrows are GPS vectors for the period 1993 to 1999. Motions are relative to station 0727, about 7 km southwest of Kuangfu. The differences between vectors indicate shortening across the valley of about 40 mm/yr.

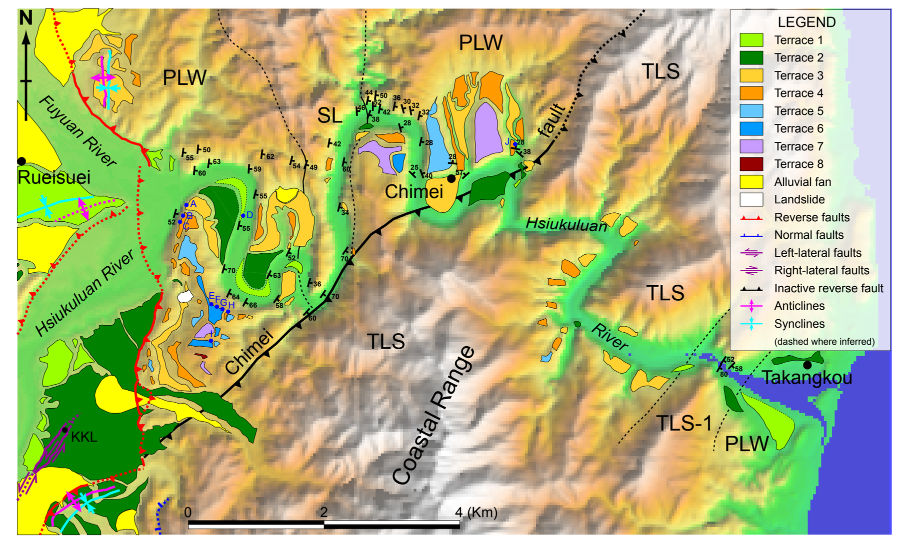

Figure B2. Since the Hsiukuluan River is the only river that flows across the Coastal Range, it provides a unique opportunity to determine the long-term rates of uplift of the range. Along the western part of its course across the range, the river has formed four deeply incised meander loops. As many as eight levels of fluvial terraces exist on both sides of the river valley. PLW: sedimentary Paliwan Formation; SL: Shuilien Conglomerate Member of the Paliwan Formation; TLS: volcanic rocks of the Tuluanshan Formation; TLS-1: a thick layer of volcanic breccia within the Tuluanshan Formation. Dark blue dots indicate where the thickness of the fluvial terrace deposit was directly measured.

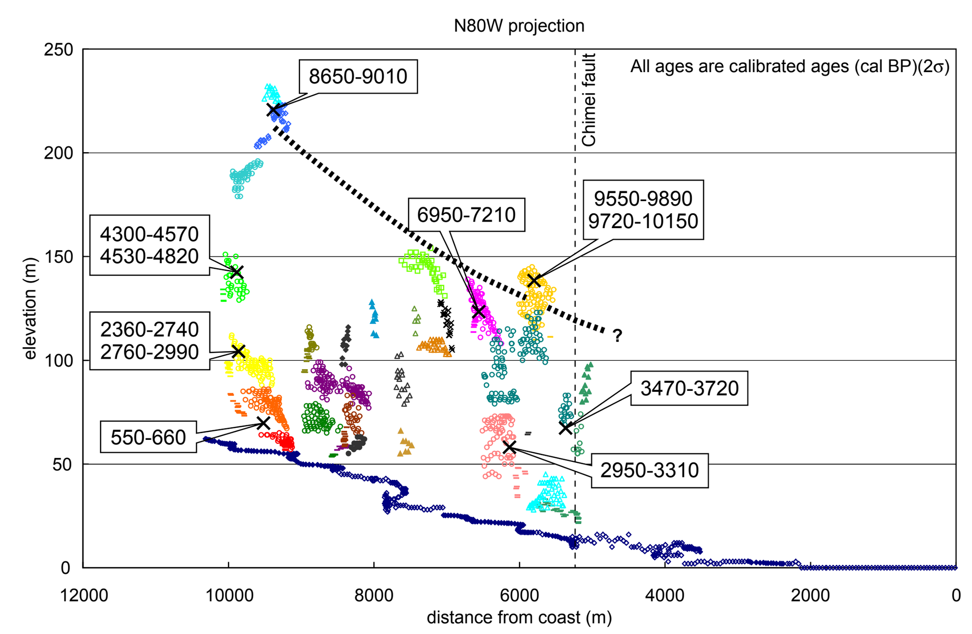

Figure B3. Preliminary correlation of river terraces along Hsiukuluan canyon. Each different color represents a different level of terraces. Solid dots represent terrace surface measurements from the DEM, and short bars represent terraces straths, measured by laser range finder. Blue dots indicate the river profile of the Hsiukuluan River. All of the terraces and the river profile were projected on to the plane in local dip direction of the bedrocks (N80W). All ages are calibrated ages (2σ), in cal BP. Our dating results and the correlation of the terraces suggests that the uplift rate of the westernmost Coastal Range is highest currently, and decreases to the east.

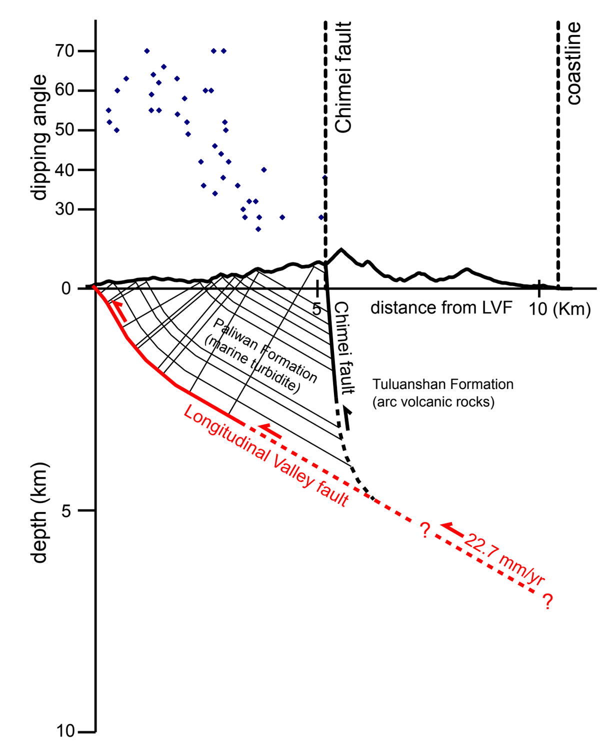

Figure B4. Reconstruction of the subsurface geometry of the Longitudinal Valley fault near Hsiukuluan canyon, from bedrock dip angles. The azimuth of the section is approximately N80W. This model indicates that the dip-slip rate along the fault is about 22.7 mm/yr and that all of the deformation is accommodated by the slip along the fault plane, with no internal deformation of the beds.

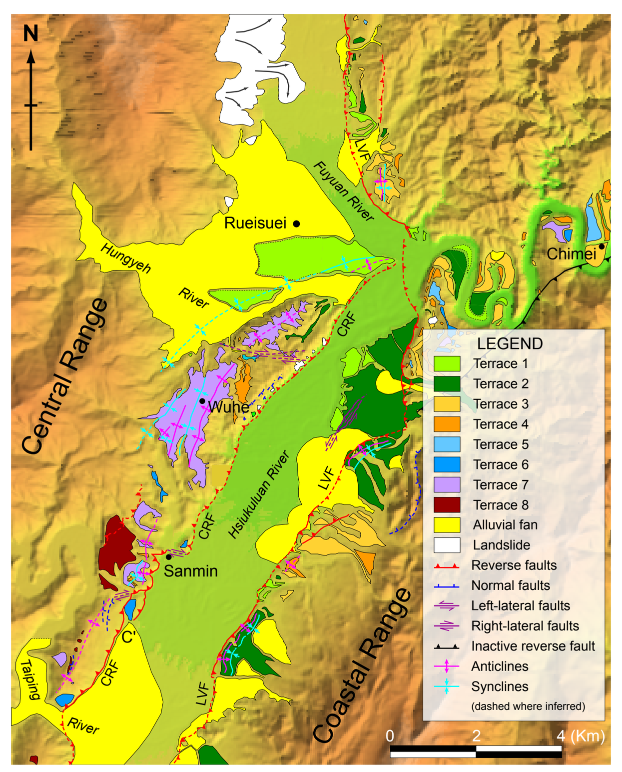

Figure B5. Detailed map of geomorphic and neotectonic features on and around the Wuhe Tableland shows deformations by young anticlines extending 13 km between the Fuyuan and Taiping Rivers. A syncline in young sediments flanks the anticlines on the northwest. These folds are formed in the hanging-wall block of the west-dipping Central Range fault (CRF). The Wuhe Tableland is a patch of uplifted lateritic fluvial terrace on the crest of a major anticline. A deformed lower and younger fluvial terrace shows that the fold extends nearly 2 km northeast of the tableland and may plunge beneath the Longitudinal Valley fault (LVF). Lateritic fluvial strath terraces along the eastern flank of the Central Range and a bedrock ridge show that the anticlines extend several kilometers southwest of the tableland.

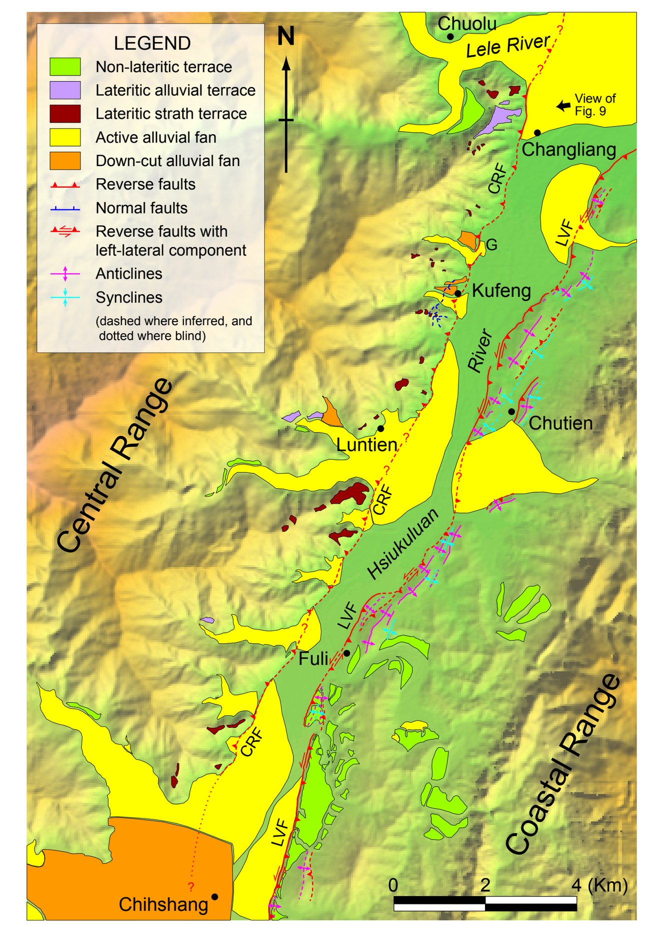

Figure B6. Detailed map of geomorphic and neotectonic features between the Lele River and Chihshang. As to the north, numerous uplifted lateritic strath terraces and deformed alluvial fans along the eastern flank of the Central Range indicate that the Central Range fault (CRF) is present along the western edge of the Longitudinal Valley. Fluvial terraces and neotectonic landforms of the east-dipping Longitudinal Valley fault (LVF), along the eastern side of the Longitudinal Valley, are also shown in the figure.

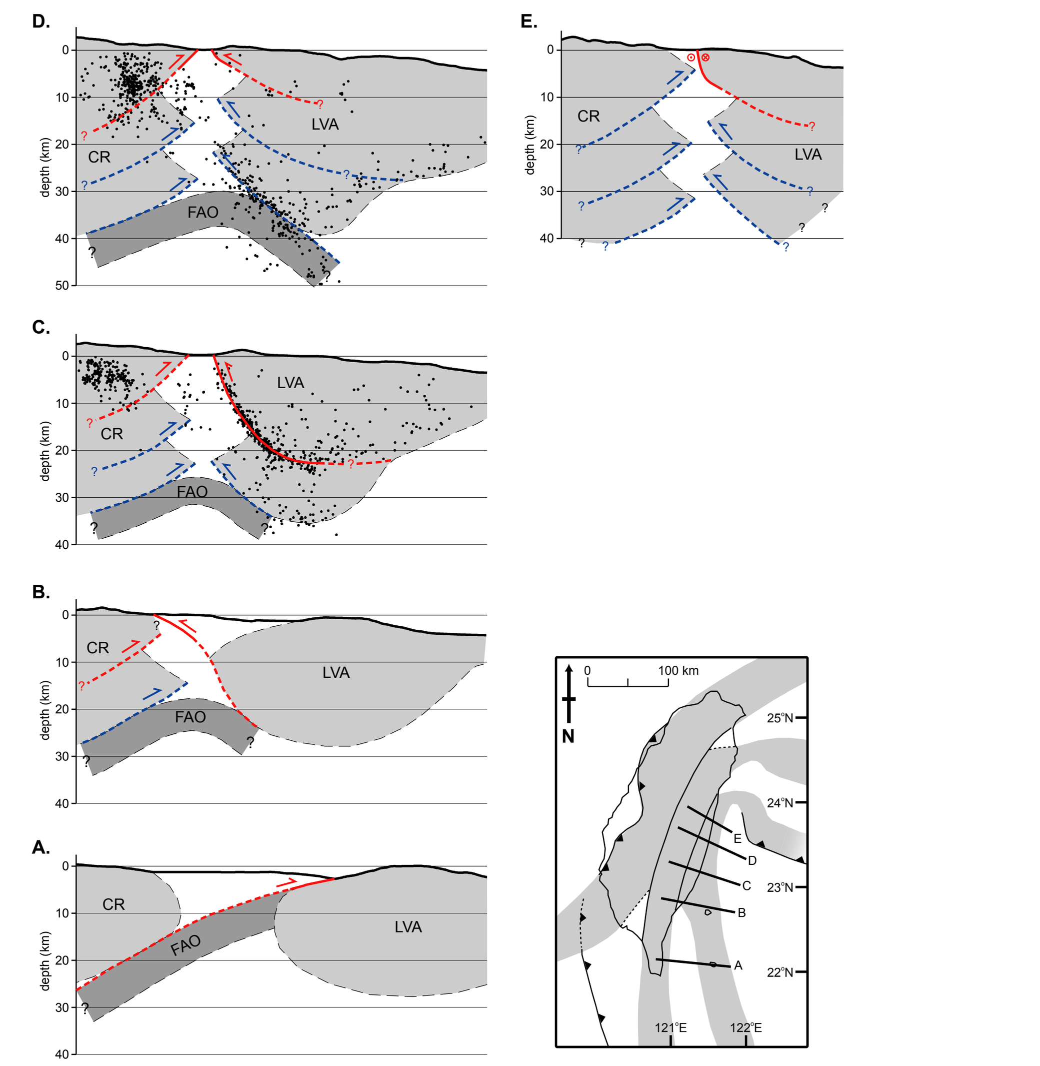

Figure B7. Schematic crustal cross-sections show our hypothesis for the evolution of the Longitudinal Valley suture. Each section is drawn using current topography and observations along the lines specified on the index map, with no vertical exaggeration. Red indicates the youngest and currently active faults in each time frame, and blue indicates older faults, which may still be active. Faults are dashed where inferred. (a) Before suturing, the Luzon forearc oceanic lithosphere (FAO) subducts beneath the Central Range continental sliver (CR). This is currently occurring at about the latitude of the southern tip of Taiwan, about 22°N. (b) As the Luzon volcanic arc lithosphere (LVA) approaches the Central Range, an east-dipping thrust fault appears, allowing the FAO to also subduct underneath the LVA. Contemporaneously on the west side of the valley, the proximity of the LVA to the CR induces formation of a newer, shallower west-dipping thrust fault above the original one. This is the current structural geometry near the southern end of the Longitudinal Valley, between about 22°40'N and 22°50'N. (c) As the suture matures, the two non-oceanic lithospheric blocks both start to thicken by evolving multiple reverse-fault wedges, with the younger ones at shallower depth. This is the current structural geometry at the latitude of Chihshang, about 23°10'N. (d) At the latitude of the Wuhe Tableland, about 23°30'N, the suture is nearing maturity. The suture has evolved into a "Christmas tree" shape, with a thick pile of sediments between the two non-oceanic lithospheric blocks and underlain by the subducted forearc oceanic lithosphere. (e) In northern Longitudinal Valley, at the latitude about 23°45'N, the dominantly sinistral Longitudinal Valley fault appears to be the only major active structure. The west-dipping Central Range fault has become inactive, and sediments in the Longitudinal Valley are lapping on the eastern flank of the Central Range.

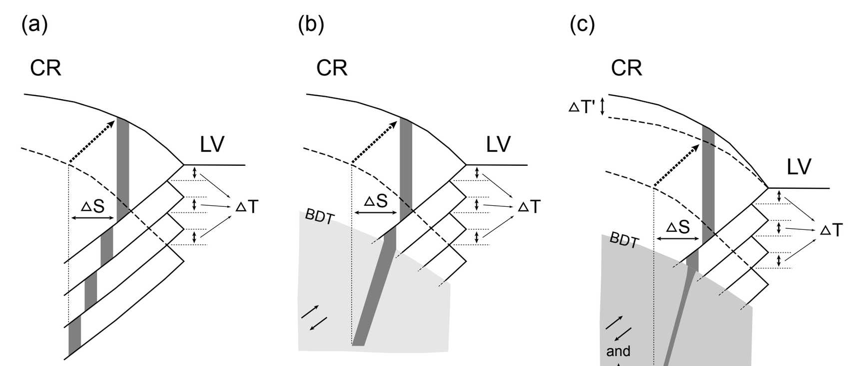

Figure B8. Cartoons show possible scenarios of crustal thickening (ΔT) and shortening (ΔS) produced by slip along the Central Range fault and by other processes. Dark gray bar indicates an originally vertical reference band. Bold dashed arrow indicates the direction of material movement. CR: Central Range; LV: Longitudinal Valley; BDT: brittle-ductile transition. (a) The Central Range fault system continues to depth, and brittle slip along the fault is responsible for all shortening and crustal thickening. (b) The Central Range fault system transforms down dip at the brittle-ductile transition into a ductile zone, where shortening and crustal thickening are accomplished by ductile simple shear. (c) Deformation occurs as in (b), but additional shortening and crustal thickening occur beneath the Central Range by pervasive pure-shear processes, which produce an arching of the upper crust ($\Delta T'$).

Acknowledgments

We greatly appreciate the assistance of C.-H. Chen, Y.-C. Chen, L.-H. Chung, C. Huang, S.-H. Huang, P.-N. Li, T. Watanuki, Y. Wang, B.C.-C. Yang, and I.-C. Yen in the field and are grateful for valuable discussions with O. Beyssac, Y.-C. Chan, H.-H. Chen, H.-T. Chu, M.-L. Hsieh, J.-C. Lee, W.-T. Liang, M.-S. Lin, R.-J. Rau, M. Simons, C.P. Stark, and S.-B. Yu. Also, we have benefited from stimulating discussions with the students of three multinational Ge122 field classes in Taiwan and a neotectonic seminar at National Taiwan University. Y.-J. Hsu and Y.-M. Wu generously provided us with their GPS and seismicity data along with valuable comments. We are grateful for financial support for our project in Taiwan from the Gordon and Betty Moore Foundation, NSF, and the Central Geologic Survey, Taiwan.